University of Stavanger

Faculty of Science and Technology

MASTER'S THESIS

Study program/Specialization: MSc Petroleum Engineering/Reservoir Engineering	Spring semester, 2013 Open access
Writer: Pål Lee Gundersen	…… (Writer's signature)
Faculty supervisor: Professor Svein M. Skjæveland External supervisor(s): Anja Eikemo Samsonsen	
Title of thesis: Compositional Simulations of Producing Oil-Gas Ratio Behaviour in Low Permeable Gas Condensate Reservoir	
Credits [ECTS]: 30	
Key words: Gas Condensate Reservoir Fluid Sampling Producing Oil-Gas Ratio Eclipse 300	Pages: 53 + enclosure: 0 Stavanger, 17 June/2013 Date/Year

Abstract

Gas condensate flow behaviour below the dew point in low permeable formations can make accurate fluid sampling a difficult challenge. The objective of this study was to investigate the producing oil-gas ratio behaviour in the infinite-acting period for a low permeable gas condensate reservoir. Compositional isothermal flow simulations were performed using a single-layer, radial and two-dimensional, gas condensate reservoir model with low permeability. The main finding in this thesis was that during a drawdown for long producing times, the producing oil-gas ratio quickly stabilized below the initial oil-gas ratio and remained almost constant throughout the infinite-acting period. The stabilization level of the producing oil-gas ratio depended on the producing rate. No previous work on the observations in this thesis has been found. A sensitivity study using two other sets of gas-oil relative permeability curves was performed, but no significant change in the producing oil-gas ratio behaviour was observed. The conclusion is that a recombined oil and gas PVT-sample from a low permeable gas condensate field could be inaccurate if the stabilized level of the producing oil-gas ratio is different from the initial oil-gas ratio.

Acknowledgements

I would like to thank my advisor Professor Svein M. Skjæveland for his guidance, support and patience throughout my study. Professor Svein M. Skjæveland has always been available to answer questions related to my work.

I wish to thank all the people in Gullfaks C, Statoil ASA in Bergen who gave me the opportunity to write this thesis in cooperation with UiS.

Thanks to Statoil ASA employees Lazaro Daniel Salem and Knut Kristian Meisingset for interesting discussions.

Contents

List of Tables

List of Figures

CHAPTER 1

1 Introduction

Gas condensate reservoirs are an important source of hydrocarbon reserves and are often found as a single phase gas at the time of discovery. During production from the reservoir, the initial reservoir pressure drops as the fluid moves towards the well. When the pressure drops below the dew point of the gas condensate, liquid starts to drop out of the gas. This is known as retrograde condensation.

Accurate fluid sampling of low permeable gas condensate reservoirs can be a challenge when the pressure drops below the dew point pressure. Thus a correct fluid composition can sometimes be very difficult to obtain. The main objective of fluid sampling is to collect a sample which represents the in-situ composition at the time of sampling. The collected fluid sample can be used to tune an equation of state (EOS) model and develop black-oil or compositional PVT tables for reservoir simulations. Inaccurate fluid sampling leads to unreliable PVT fluid data and field production forecasts and recovery estimations become highly uncertain.

Reudelhuber (1957) described challenges and procedures for collecting fluid samples for saturated and undersaturated oil reservoirs. It was suggested that challenges related to reservoir fluid sampling could be avoided or minimized if the fluid samples were collected early in the production life of the reservoir.

Bøe et al. (1989) presented analytical solutions which showed that for long producing times, the GOR was constant during a drawdown test in the infinite-acting period for solution-gas-drive reservoirs. The study was limited to radial flow with a fully penetrating vertical well in the center of the drainage area. Results showed that the stabilization level of the GOR would depend strongly upon the rate and could be higher or lower than the initial GOR.

Peres et al. (1990) used a black-oil simulator to estimate the bubble point pressure of a fluid sample obtained from a solution-gas-drive reservoir. Results showed that the recommended well sampling procedures from Reudelhuber (1957) and RP 44 (2003) did not

always yield bottomhole fluid samples that represented the in-situ fluid composition. Thus, issues with standard well conditioning procedures obtained in the work of Peres et al. (1990) would also extend to gas condensate reservoirs. Peres et al. (1990) also observed that the producing GOR remained constant during the first flow period as long as the flow rate remained constant during the infinite-acting period. This was the case even though the gas saturation was higher than the critical gas saturation. These results seemed to be consistent with the analytical results presented by Bøe et al. (1989).

MCain Jr et al. (1992) performed compositional simulations with different retrograde gas condensates using a radial reservoir model. Results showed it was possible to obtain an accurate recombined surface sample even though the BHFP was less than the dew point pressure of the initial reservoir fluid. Fluid sampling should be performed early in the life of the well and at low production rate. McCain Jr et al. (1992) also concluded that at high production rates, the producing GOR could appear to be constant when the composition of the production stream was not representative of the original reservoir gas.

Thomas et al. (1996) discussed how the gas-oil ratio (GOR) varied with the production flow rate for a gas condensate reservoir. Low flow rates might not provide sufficient lift to transport the condensed liquid from the reservoir and into the wellbore. In that case liquid hold-up would increase and slugging might occur in the well. Thus the GOR would increase. At high flow rates, the liquid drop out could be induced and the produced wellstream would contain less liquid and the GOR would increase. It was suggested that the separator GOR could be too high depending upon whether the well was produced with too high or too low flow rates. There would also be an optimal producing flow rate for the well in question.

El-Banbi et al. (2001) used a compositional simulator to investigate a recommended sampling procedure for volatile oil reservoir fluids. Results showed it was more likely to obtain a correct fluid sample early in the production lifetime of the well and at low production rate. In addition a correct fluid sample of a volatile oil reservoir could be taken even if the flowing well BHP was less than the bubble point pressure of the initial fluid.

Whitson et al. (2012) performed numerical modeling of wells in liquid rich shale (LRS) fractured reservoirs with ultra low permeability (1E-05 to 0.001 mD). Fully implicit black-oil and compositional models produced approximately equal results. Observations showed that the liquid yield (producing OGR, r_p) remained almost constant for an extended period of time (months or years) for all LRS oil and gas wells if the flowing BHP was approximately constant.

This seemed to be the analytical solution for LRS flow at infinite-acting conditions for 1D linear flow in planar fractures. Another conclusion was that the producing OGR for gas condensate LRS reservoirs was equal to the solution OGR evaluated at current flowing BHP. ($r_p \approx r_s (p_{wf})$). A recommended sampling strategy for LRS reservoirs was to collect the sample early with minimal drawdown.

An accurate recombination of the producing oil-gas ratio (r_p) is important in order to avoid large deviations in future well predictions. An interesting question is whether the producing oil-gas ratio might stabilize on different levels, depending on the production rate. The producing oil-gas ratio might stabilize too high or too low from the initial oil-gas ratio (r_i) as has been discussed in previous publications.

In this study, the behaviour of the producing oil-gas ratio of a rich gas condensate fluid in the infinite acting period is investigated. Test cases with a sequence of constant rates and two schematic flow-rate sequences with changing rates are simulated. A single-layer, radial, two-dimensional and compositional reservoir model is used. A single vertical well is located at the center of the reservoir model. The reservoir model is considered homogeneous and capillary forces, gravity effects, skin and non-Darcy effects and are neglected. Constant fluid composition with depth is considered throughout the formation height.

Chapter 2 reviews different types of reservoir fluids and addresses the gas condensate flow behaviour. Differences between a black-oil and compositional PVT simulator and general fluid sampling are explained. Chapter 3 describes the reservoir model and simulation preparations. Chapter 4 presents simulation results and Chapter 5 ends with discussions and conclusions.

CHAPTER 2

2 Theory

2.1 Classification of Reservoir Fluids

Hydrocarbon fluids are divided into five main types: dry gas, wet gas, gas condensate, volatile oil and black-oil (McCain, 1990). The phase behaviour of a reservoir fluid at surface and reservoir conditions will depend on the fluid composition, pressure and temperature. Typical compositions of different hydrocarbon fluids are given in **Table 1**.

Table 1: Typical composition and properties of reservoir fluids (Wall, 1982).

Component	Black-Oil	Volatile Oil	Condensate	Gas
Methane	48.83	64.36	87.07	95.85
Ethane	2.75	7.52	4.39	2.67
Propane	1.93	4.74	2.29	0.34
Butanes	1.60	4.12	1.74	0.52
Pentanes	1.15	2.97	0.83	0.08
Hexanes	1.59	1.38	0.60	0.12
C_{7+}	42.15	14.91	3.80	0.42
Molecular wt C_{7+}	225	181	112	157
Gas-Oil Ratio SCF/B	625	2000	18200	105000
Liquid-Gas Ratio b/MMSCF	1600	500	55	9.5
Tank oil gravity API	34.3	50.1	60.8	54.7
Color	Green/black	Pale red/brown	Straw	White

The best reservoir fluid characterization is performed in a laboratory. Yet, available information during production such as the initial producing gas-oil ratio, stock-tank liquid gravity and fluid color might be sufficient fluid indicators. A typical retrograde gas condensate fluid exhibit gas-oil ratios (GOR's) between 3000 and 150.000 scf/STB and oil-gas ratios (OGR's) from about 350 to 5 STB/MMscf (Whitson and Brulé, 2000). **Figure 1** shows a range of reservoir fluids with corresponding OGR and GOR values.

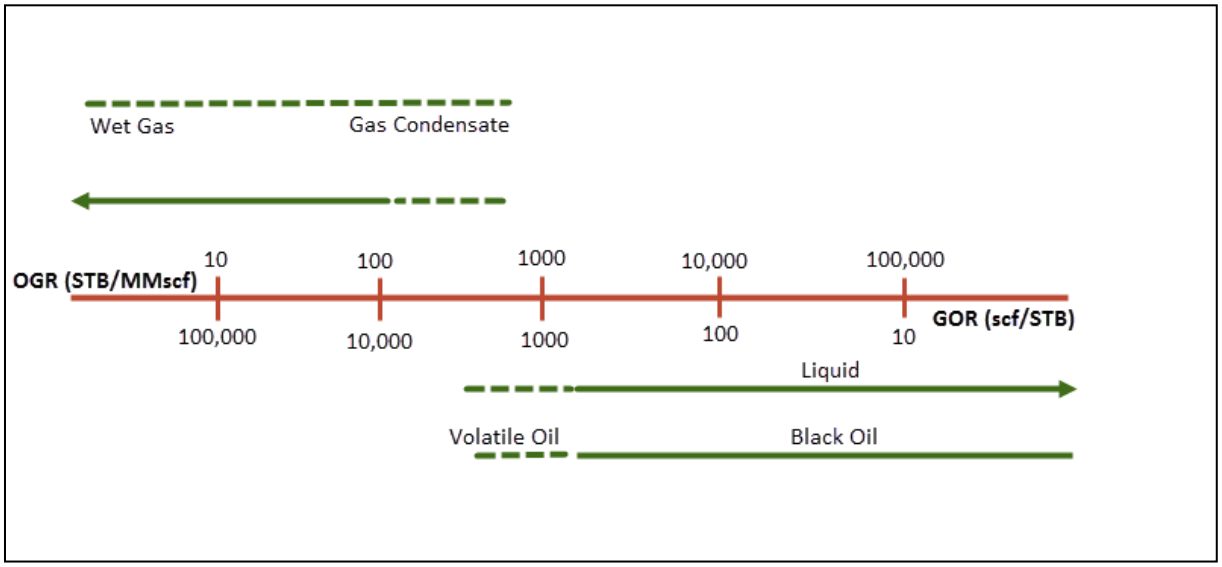

Figure 1: Spectrum of reservoir fluids with corresponding OGR and GOR values (Whitson & Brulé, 2000)

The following two criteria can be used to characterize a reservoir fluid in a typical pressure-temperature (P-T) diagram:

1) The location of the reservoir temperature (T_{res}) relative to the cricondentherm (T_{cri}) and the critical temperature (T_c)
2) If the pressure and temperature of standard conditions (P_{sc} and T_{sc}) are inside or outside of the two-phase region in the P-T diagram

The P-T diagram illustrated in **Figure 2** shows four types of depletion reservoirs for the same hydrocarbon system.

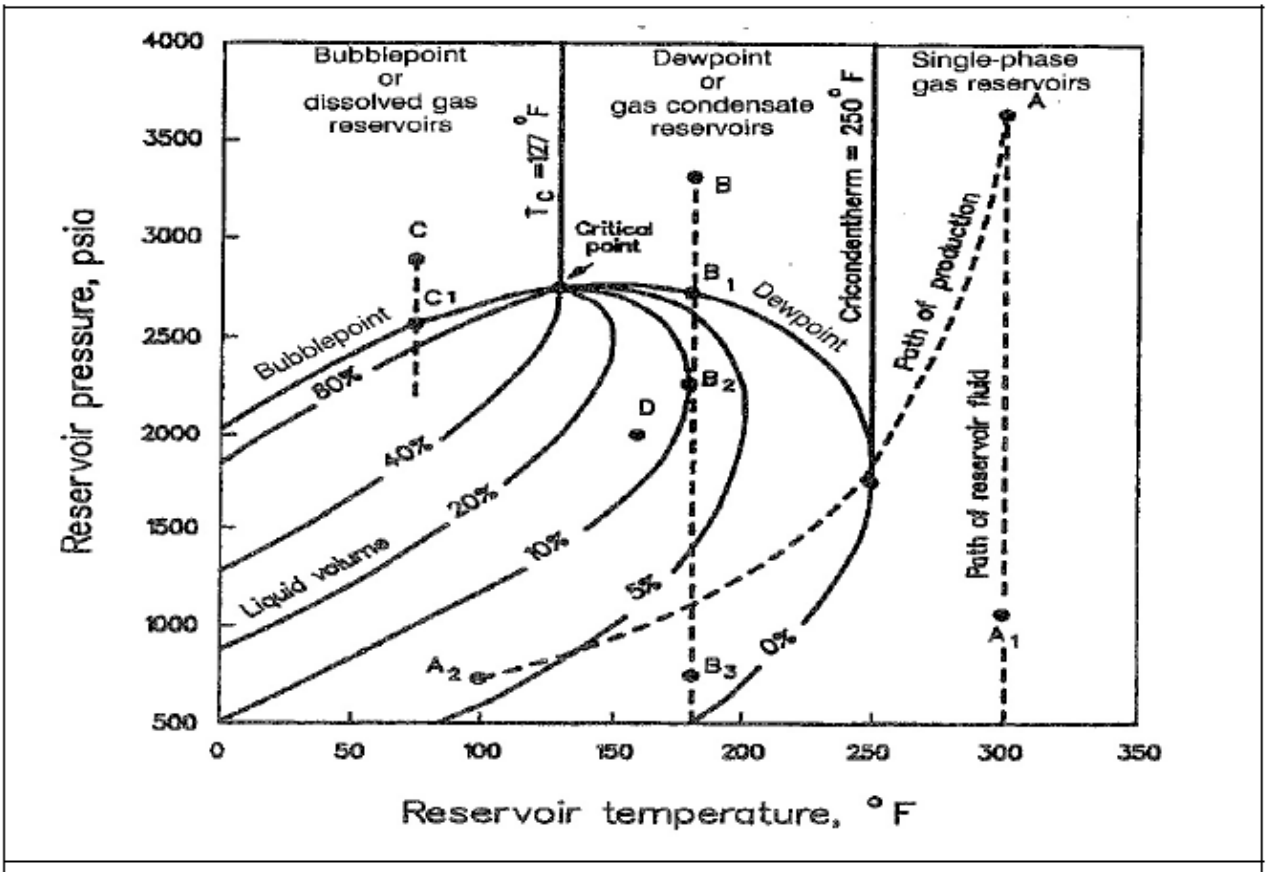

Figure 2: P-T diagram with different types of depletion reservoirs (Whitson & Brulé, 2000).

The two-phase region consists of a bubble point curve and a dew point curve. The critical point is located where the bubble point curve and dew point curve intersect. The properties of gas and liquid mixtures become identical at the critical point. The bubble point (point C_1 in **Figure 2**), is the pressure at which the first bubble of gas vaporizes out of solution from the reservoir oil. In the case of retrograde gas condensate depletion, the dew point (point B_1 in **Figure 2**) is reached when the first drop of liquid condenses from the reservoir gas phase.

Dry Gas

Dry gases consist of methane and non-hydrocarbons such as nitrogen and carbon dioxide (Danesh, 1998). A dry gas remains single phase from reservoir to separator conditions and will follow the path from point A to A_1 in **Figure 2**. A reservoir fluid is classified as dry gas if the reservoir temperature is greater than the cricondentherm and if surface conditions are outside the two-phase envelope. The word "dry" means that the gas does not contain sufficient heavy molecules to create hydrocarbon liquid at the surface.

Wet Gas

A reservoir fluid is defined as wet gas if the reservoir pressure is larger than the cricondentherm and the surface conditions are inside the two-phase region. A dry gas is mainly composed of methane and other light components. It can sometimes be difficult to distinguish between a dry and wet gas, because any gas can be cooled down enough to condense into a liquid phase (Whitson & Brulé, 2000).

Retrograde Gas Condensate

An isothermal decrease in pressure is illustrated by the points B, B1, B2 and B3 in **Figure 3.** When the reservoir pressure is larger than the dew point of the fluid, the fluid will remain single-phase gas and the producing GOR is constant. This is illustrated between point A and point A1 in **Figure 3**. As the reservoir pressure drops below the dew point (point B1 in **Figure 3**) liquid starts to drop out in the reservoir. The liquid will not flow until the accumulated condensate saturation exceeds the critical condensate saturation (S_{cc}). An even further pressure reduction will cause the liquid to revaporize. A revaporization can be observed in a PVT-cell experiment but is less likely to occur during actual field production (McCain, 1990). The reservoir temperature must be larger than the critical temperature and less than the cricondentherm.

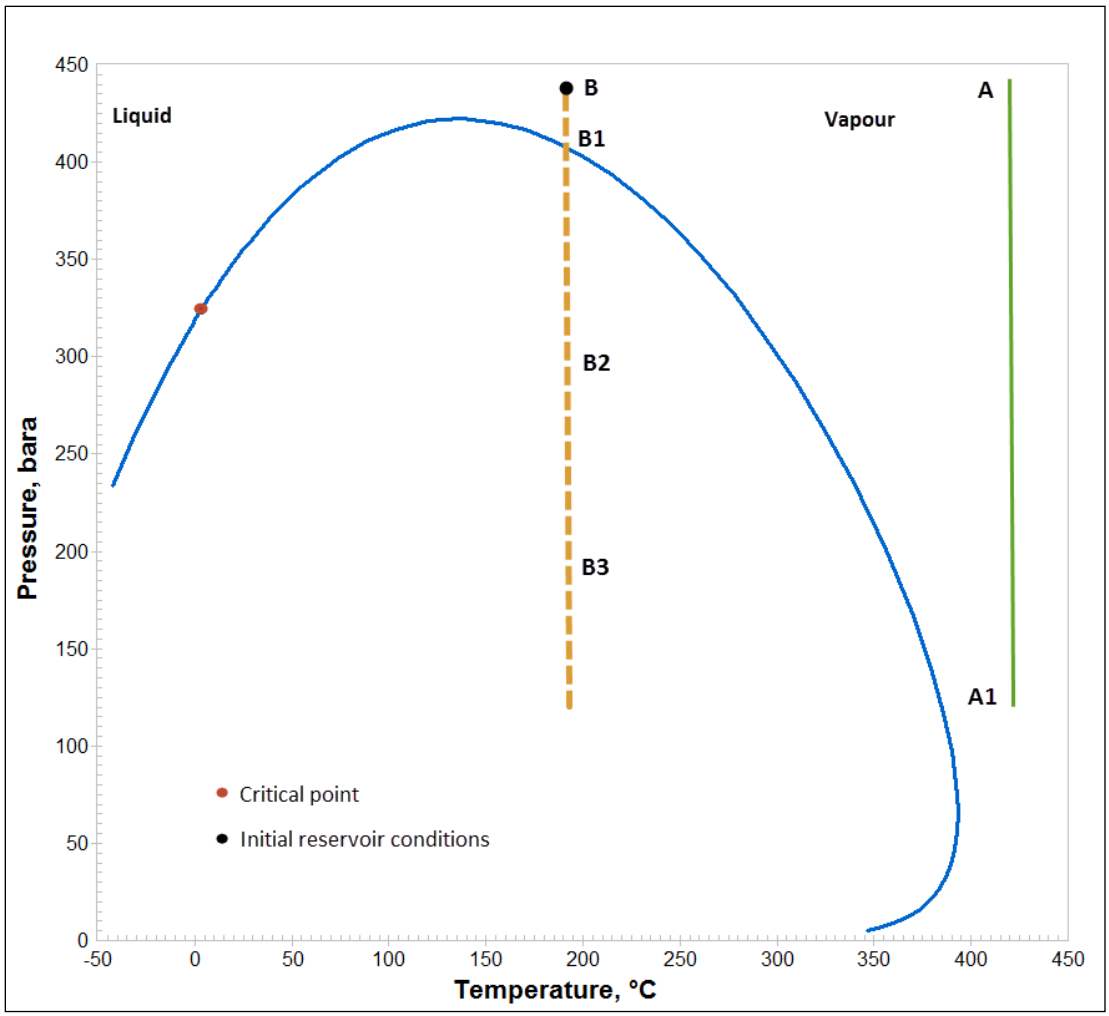

Figure 3: P-T diagram of a typical retrograde gas condensate system

Volatile Oil and Black-Oil

A volatile oil contains fewer heavy molecules and more intermediate components (ethane through hexane) than a black-oil (McCain, 1990). The critical temperature of a volatile oil is less than for a black-oil and is closer to the reservoir temperature. Small pressure reductions below the bubble point can cause large changes in the volatile oil properties. As an extreme case, the oil volume may shrink by 50% with a pressure reduction of 100 psia below $p_{b.}$ (Whitson and Brulé, 2000). On the other hand, black-oil exhibits properties that experience a nearly linear pressure relationship as the pressure is reduced below bubble point. A reservoir fluid is classified as a volatile oil if the reservoir temperature is less than the critical temperature.

2.2 Flow Regimes and Drawdown Behaviour of Gas condensate

Fevang (1995) identified three flow regions related to drawdown flow behaviour in gas condensate reservoirs:

- Region 1: An inner near-wellbore region where two phases (oil and gas) flow simultaneously at different velocities.

- Region 2: A region of condensate buildup where the mobility of liquid condensate is (practically) zero and only gas flows.

- Region 3: A region which contains only single phase gas (original reservoir gas).

Figure 4 shows the oil saturation distribution around the wellbore for a drawdown simulation below the dew point of the gas condensate reservoir model used in this study.

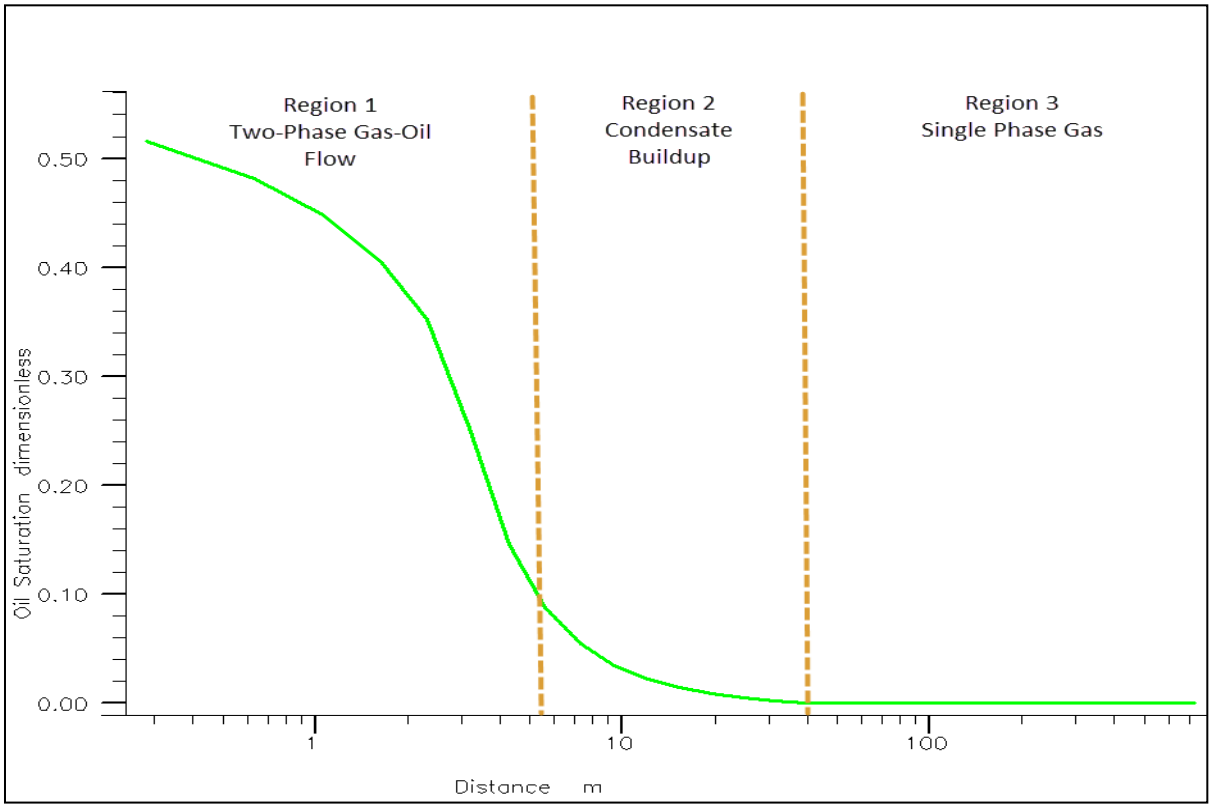

Figure 4: Condensate buildup in the 2D, radial reservoir model during a drawdown in Eclipse 300.

Region 1

Region 1 is closest to the wellbore. The oil saturation is larger than the critical condensate saturation (S_{cc}) and both oil and gas flow in Region 1. The flowing composition (GOR) is almost constant throughout Region 1. The single-phase gas that enters Region 1 is equal to the composition of the produced wellstream. It is possible to determine the flowing composition within Region 1 as long as the produced wellstream is known. The dew point of the producing wellstream is equal to the reservoir pressure ($p_d = p_{res}$) at the outer edge of Region 1. The deliverability loss in gas condensate wells will mainly depend on the gas relative permeability in Region 1. Due to condensate buildup, the gas relative permeability is drastically reduced in this region. The relative permeability of gas is mainly a function of the liquid saturation distribution. The richness of the flowing wellstream and the PVT properties of the reservoir gas will determine the amount of liquid saturation in Region 1. The difference in the solution oil-gas ratio, $\Delta r_{s,}$ between the gas entering Region 1 and the gas flowing at a given radial distance, is equal to the amount of condensate flowing in Region 1. Because OGR decreases with pressure the amount of condensate will increase towards the wellbore.

Region 2

Region 2 is the intermediate zone where condensate dropout begins. The condensate buildup occurs because the pressure drops below the dew point pressure of the reservoir fluid. The pressure drops due to 1) The pure decline in the bulk of the reservoir and 2) The pressure gradient imposed on the flowing gas in Region 2. The condensate saturation is below the critical condensate saturation and only gas flows in Region 2. The oil mobility is zero (or very low). When the single phase gas from Region 3 enters Region 2, the first droplets of liquid condense from the original reservoir gas. Thus, the dew point pressure of the original reservoir gas is in the boundary between Region 2 and Region 3. Whitson and Thorp (1983) showed that the condensate saturation during pure pressure depletion could approximately be determined by the liquid drop out from constant volume depletion (CVD) (Corrected for initial water saturation). Gas from Region 2 will contain less heavy components due to the loss of condensed liquid. Consequently the gas leaving Region 2 is leaner compared to gas entering Region 2. The size of Region 2 decreases with time since

Region 1 is expanding. Region 2 will therefore be largest early on, prior to the reservoir pressure falling below the dew point.

Region 3

Region 3 only exists for an undersaturated gas condensate reservoir and the reservoir pressure in Region 3 is greater than the dew point of the original gas. Thus only single phase gas will be present.

Coexistence of Flow Regions

As long as the flowing bottomhole pressure (FBHP) is less than the dew point pressure of the original reservoir gas, Region 1 will always (and only) exist throughout the reservoir. Region 2 will always exist together with Region 1 after the reservoir pressure drops below the dew point. Region 3 will in this case not exist anymore. After steady state condition is reached, it is not possible for Region 2 and Region 3 to exist in the absence of Region 1. For very rich gas condensate, Region 2 and Region 3 might be absent and only Region 1 will be present throughout the whole drainage area. **Table 2** summarizes the valid conditions of the three different flow regions proposed by Fevang (1995).

Table 2: Coexistence of flow regions, Fevang (1995).

Pressure condition	**Region number**		
	1	**2**	**3**
$p_{wf} > p_d$			X
$p_{res} < p_d$	X	(X)	
$p_{wf} < p_d$ and $p_{res} > p_d$	X	(X)	X
X exist (X) may exist			

Fevang and Whitson (1995) proposed three different pseudo-pressure integrals corresponding to the three flow regions and are described as follows:

Total
$$\Delta p_p = \int_{p_{wf}}^{p_{res}} \left(\frac{k_{rg}}{B_{gd}\mu_g} + \frac{k_{ro}}{B_o\mu_o}R_s\right)dp = \quad (1)$$

Region 1
$$\int_{p_{wf}}^{p^*} \left(\frac{k_{rg}}{B_{gd}\mu_g} + \frac{k_{ro}}{B_o\mu_o}R_s\right)dp +$$

Region 2
$$\int_{p^*}^{p_d} \frac{k_{rg}}{B_{gd}\mu_g}dp +$$

Region 3
$$k_{rg}(S_{wi}) \int_{p_d}^{p_{res}} \frac{1}{B_{gd}\mu_g}dp$$

The upper and lower pressure limits in Region 1 are defined as the outer boundary pressure, p^*, and the flowing bottomhole pressure, p_{wf}, respectively. The dew point of the gas that enters Region 1 is equal to p^*, since only single phase gas flows into Region 1. In Region 2, p_d is the initial dew point pressure at the outer boundary if $p_{res} > p_d$, or it will be the average reservoir pressure if $p_{res} < p_d$. The pressure integral in Region 3 will only exist if the initial reservoir pressure is larger than the dew point pressure. Thus the upper and lower pressure limits in Region 3 are p_{res} and p_d, respectively.

2.3 Black-Oil and Compositional Reservoir Simulation

During drawdown of a gas condensate reservoir, the wellstream composition does not change significantly when the reservoir pressure is larger than the dew point pressure of the fluid. A larger change in the composition of the producing wellstream is expected when the reservoir pressure decreases below the dew point. This is due to the retrograde condensate drop out in the reservoir. A black-oil simulation model might not give accurate results when the component exchange between the oil and gas phase becomes more complex. An example is when gas is injected into an oil reservoir. A compositional reservoir simulator can model the component exchange between gas and liquid phase more accurately. Coats (1985) showed that black-oil simulators could be used for gas cycling in gas condensate reservoirs above the dew point. These findings were supported by Fevang et al. (2000) for lean to medium rich gas condensate fluids.

The mathematical complexity of an EOS is larger than a simple black-oil PVT formulation in a reservoir simulator (Whitson et al., 1999). Thus, a compositional simulator usually runs slower than a black-oil simulator. A compositional reservoir model uses an EOS with a reduced number of components. This is mainly due to the CPU and memory limitations in the compositional simulator. The reduction in components is called pseudiozation or lumping. A fluid characterization procedure in PVT simulations often divides the fluid composition in 13 to 30 pseudocomponents. A pseudocomponent can be a pure component like methane or a group of components. The number of components in an EOS characterization depends not only on computational restraints, but also on the desired level of accuracy from the EOS. A stepwise pseudoization procedure has been recommended by Whitson et al. (2000).

Another important distinction between a black-oil and compositional simulator is the selected method of compositional gradients. A compositional gradient in a black-oil model is defined by the solution GOR (R_s) versus depth variation for an oil zone and the solution OGR (r_s) versus depth variation in a gas zone.

The black-oil mass balance equations for oil and gas flow respectively can be written as:

$$\nabla \cdot \left[\left(\frac{r_s k_{rg}}{\mu_g B_g} + \frac{k_{ro}}{\mu_o B_o}\nabla p\right)\right] = \frac{\varphi}{k}\frac{\partial}{\partial t}\left(\frac{r_s S_g}{B_g} + \frac{S_o}{B_o}\right) \quad (2)$$

and

$$\nabla \cdot \left[\left(\frac{R_s k_{ro}}{\mu_o B_o} + \frac{k_{rg}}{\mu_g B_g}\right)\nabla p\right] = \frac{\varphi}{k}\frac{\partial}{\partial t}\left(\frac{R_s S_o}{B_o} + \frac{S_g}{B_g}\right) \quad (3)$$

where $S_o + S_g + S_{iw}$= 1, R_s= gas dissolved in the oil-phase and r_s = oil dissolved in the gas phase. The term r_s is included to make the system of equations applicable to gas condensate reservoirs.

In a compositional model, key fluid parameters like density ρ and viscosity μ are in addition to pressure dependent on the fluid composition and can be written as:

$$\rho_o = \rho_o(p_o, x_1, \ldots, x_{nc})$$

$$\rho_g = \rho_g(p_g, y_1, \ldots, y_{nc})$$

where x_{nc} and y_{nc} represent components of liquid and vapor respectively.

Equation of State (EOS)

Equations of states (EOS) are mathematical relations between pressure, volume and temperature (Whitson and Brulé, 2000). An EOS can accurately describe the phase behaviour for pure substances and mixtures.

Since the first introduction of van der Waals EOS in 1873, many cubic EOS have been proposed in the literature. Two widely used cubic EOS are summarized below.

- Soave-Redlich and Kwong (SRK) equation of state (1972)

$$P = \frac{RT}{v-b} - \frac{a(T)}{v(v+b)} \tag{4}$$

The constants a and b are "attractive" and "repulsive" forces between molecules respectively, *T* = temperature, *R* = universal gas constant and *v* = molar volume. The SRK EOS overestimates liquid volumes and underestimates liquid densities of petroleum mixtures.

- Peng-Robinson (PR) equation of state (1976)

$$P = \frac{RT}{v-b} - \frac{a(T)}{v(v+b)+b(v-b)} \tag{5}$$

The Peng-Robinson EOS improved the liquid density predictions in particular compared to the Soave-Redlich and Kwong EOS.

To perform EOS calculations, the minimum input data are molar composition, molecular weight, and specific gravity of the heaviest components (Whitson et al., 1999). With this input as a minimum requirement, an EOS can calculate (practically) any phase and volumetric properties. In other words, bubble point/dew point at specified temperature, P-T diagrams, densities, Z-factors, separator GOR and surface gravity can be determined.

2.4 Fluid Sampling

Accurate fluid sampling is necessary to determine the PVT behaviour and properties of a reservoir fluid. The main objective of reservoir fluid sampling is to gather a fluid sample which represents the original reservoir fluid at the time the sample was collected (API RP 44., 2003). Inaccurate fluid characterizations cause's large deviations of volumes in-place estimates and recovery predictions. (Nagarajan et al., 2006).

Two fluid sampling methods used in the petroleum industry are bottomhole sampling and surface sampling. Bottomhole samples are collected at reservoir conditions. A sampling device is lowered down to a pre-selected depth and collects the desired sample directly from the producing wellstream. The sampler is brought to surface conditions, where the fluid sample is re-pressured and restored to a single-phase and eventually brought to the laboratory for further analysis. In a surface sampling method, a set of separator gas and oil samples is collected after the well maintains stable flow conditions. Separator fluids are recombined at the producing gas-oil ratio (GOR). Prerequisites for an accurate surface sampling are correct determinations of oil and gas flow rates in addition to properly calibrated equipment.

Recommended sampling guidelines published by API RP 44 (2003) suggest a continuous rate reduction of 30 to 50% until a trend in the GOR is established. The following guidelines were also proposed:

1) If the GOR still remains constant after the first rate reduction, there might be flow of undersaturated fluid into the wellbore. The phase condition and composition of the reservoir fluid has remained unchanged and the well is ready for sampling.

2) If the GOR decreases after the first rate reduction, the presence of free gas around the wellbore might be indicated. In this case it is recommended to perform the well-conditioning in stages by letting the well flow at new reduced rates until GOR stabilizes. The free gas might develop either as a result of coning from a gas cap or that the flowing bottomhole pressure is less than the fluid saturation pressure.

3) If the GOR increases it might indicate simultaneous production of oil and gas from oil and gas-bearing formations. The increase in GOR could also indicate a subsidence of an oil cone.

CHAPTER 3

3 Preparation of Simulation Experiments

3.1 Reservoir Model

A single-layer, radial, 2D and homogeneous reservoir model was used to investigate the producing OGR behaviour in the infinite-acting period. A fully perforated vertical well was located at the center of the reservoir model. The reservoir model consisted of 30 grid blocks increasing logarithmically with radius away from the wellbore. Gravity effects, capillary forces, skin factor and non-Darcy effects were neglected. The reservoir model was initially saturated only with a gas condensate fluid with constant composition with depth. The reservoir properties and reservoir grid distribution of the gas condensate reservoir model are listed in **Table 3** and **Table 4**, respectively. **Figure 5** shows the top view of the gas condensate reservoir model.

Table 3: Reservoir properties used in the compositional simulations.

Reservoir porosity, φ	20 %
Absolute (horizontal and vertical) permeability, k	5 mD
Reservoir thickness, h	25 m
Total reservoir radius, r_e	914.2 m
Well radius, r_w	0.10 m
Initial reservoir pressure, p_{res}	425 bar
Reservoir temperature, T_{res}	110°C
Irreducible water saturation, S_{wi}	0 %
Reservoir drainage area, A	$2.626 \cdot 10^{6}$ m^2
Rock compressibility, C_{rock}	$5.075 \cdot 10^{-5}$ bar
Skin factor, S	0

Table 4: Grid size distribution of the 2D, radial reservoir model used in simulations.

Inner Most Grid Radius, [m]	0.20
Reservoir Grid Cell Size in Radial Direction, [m]	0.2512 0.3155 0.3963 0.4977 0.6252 0.7852 0.9862 1.2387 1.5558 1.9541 2.4544 3.0827 3.8719 4.8631 6.1081 7.6718 9.6358 12.1026 15.2009 19.0924 23.9802 30.1192 37.8299 47.5146 59.6786 74.9567 94.1460 118.2479 148.5200 186.5419

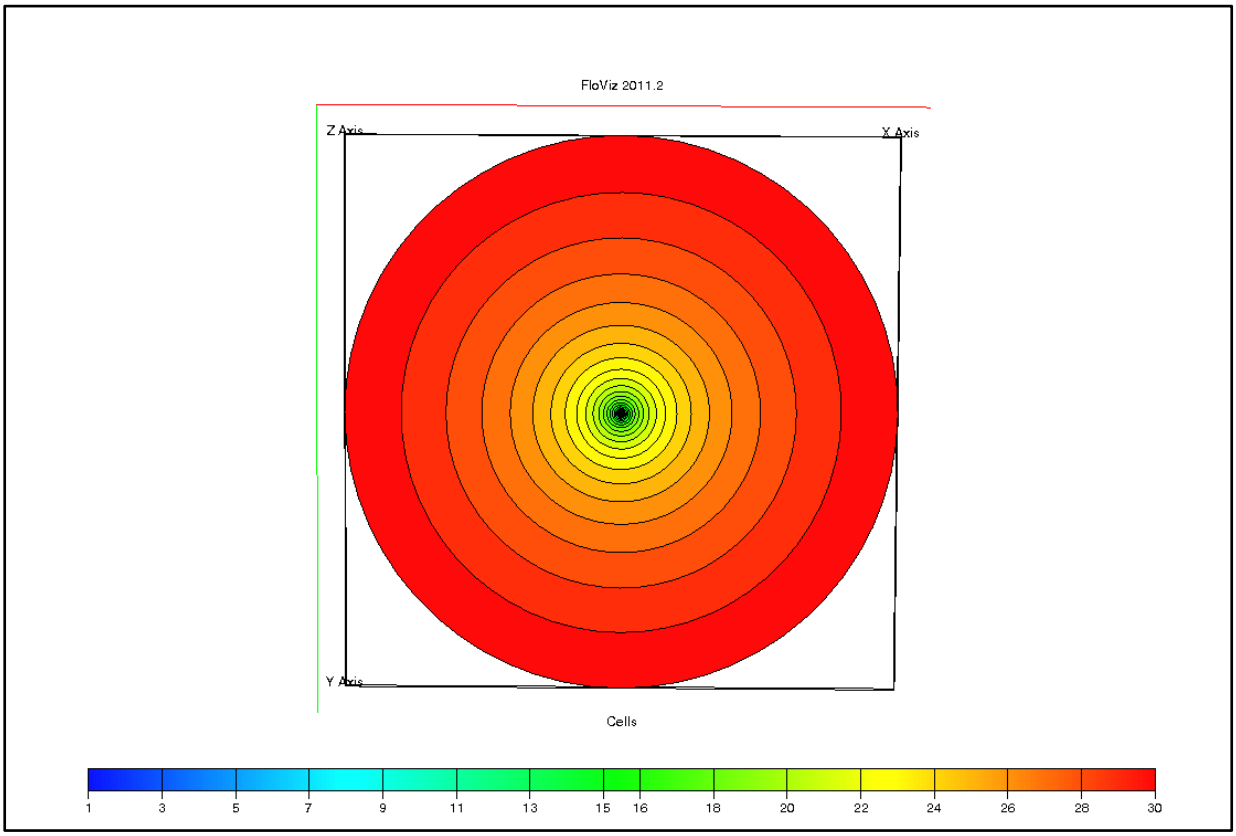

Figure 5: Top view of the 2D, radial compositional gas condensate reservoir model used in the simulations.

3.2 Generation of Compositional PVT data

A gas condensate fluid was sampled in a reservoir from field Alpha. Initial fluid characterization in PVTsim for Eclipse 100 showed an acceptable match between measured and simulated PVT data. It was necessary to generate new PVT input data for the Eclipse 300 simulations. The initial 22-component fluid was lumped to 8 components which are presented in **Table 5**. The new pseudozation showed good agreement between measured and simulated PVT data with 22 and 8 components. The Soave-Redlich and Kwong (SRK) equation of state and the Lohrenz, Bray and Clark correlation was used in PVTsim to generate Eclipse 300 input data. The simulated dew point pressure in PVTsim was 418.8 bar and Eclipse 300 reported a saturation pressure of 417.05 bar. A constant-volume depletion of the 8-component fluid was simulated in PVTsim. The liquid drop out simulation in PVTsim is given in **Figure 6**.

Table 5: Reservoir fluid composition used in the simulations.

Component	Mol %	T_c [°C]	p_c [bar]
$C_1 + N_2 + CO_2$	75.323	-79.291	46.84
$C_2 + C_3$	11.728	61.371	45.95
C_4-C_6	4.612	187.291	34.03
C_7-C_9	3.845	281.721	29.63
C_{10}-C_{15}	2.648	360.466	20.6
C_{16}-C_{22}	1.192	449.479	15.51
C_{23}-C_{33}	0.525	541.29	13.49
C_{34}-C_{80}	0.128	713.447	12.31

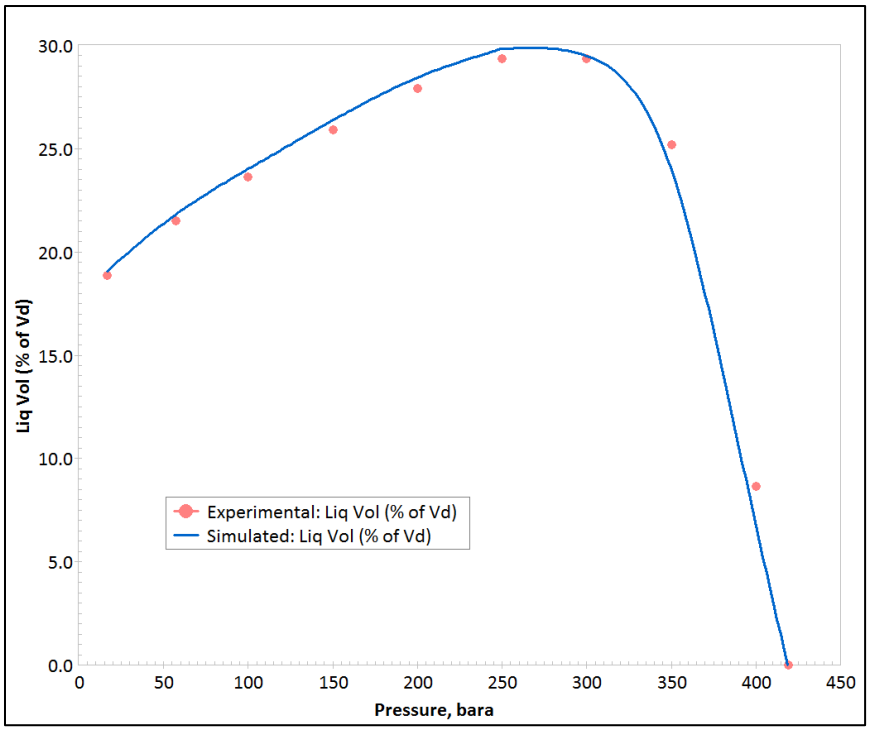

Figure 6: Simulated liquid drop out of the 8-component gas condensate in PVTsim.

3.3 Single-Phase Pseudo-Pressure

Al Hussainy et al. (1966) showed that the basic differential equation for radial flow could be approximately linearized for the flow of a real gas in a porous media by introducing the real gas pseudo-pressure:

$$m(p) = 2 \int_{p_{wf}}^{p} \frac{p}{\mu_g z_g} dp \tag{6}$$

Values of real gas pressure, gas viscosity and single gas Z factor of the gas condensate fluid were created from a CVD simulation in PVTsim. Eq. (6) was evaluated using the trapezoidal rule as follows:

$$m(p) = 2 \sum_{i=2}^{n} \frac{1}{2} [(\frac{p}{\mu Z})_{i-1} + (\frac{p}{\mu Z})_i] \cdot (p_i - p_{i-1}) \tag{7}$$

Values of m(p) as a function of the real pressure were calculated and are listed in **Table 6**. **Table 6** was used to convert the real gas pressure to pseudo-pressure for a gas well drawdown test analysis described in section 3.4 of this chapter. A graph of the values of m(p) versus pressure, corresponding to **Table 6,** is presented in **Figure 7.** It was assumed that for high pressures, in excess of 8000 psia, the pseudo-pressure function was almost linear and could be described by:

$$m(p) = 142767p + 7 \cdot 10^8 \left[\frac{psia^2}{cP}\right] \tag{8}$$

The expression in Eq. (8) was used when the model validity was tested.

Table 6: Generation of the real gas pseudo-pressure as a function of the real pressure using the trapezoidal rule.

$p\ [psia]$	Z_g	$\mu_g\ [cP]$	$\frac{2p}{\mu Z}$	$\overline{\frac{2p}{\mu Z}}$	Δp	$\overline{\frac{2p}{\mu Z}} \cdot \Delta p$	$m(p) = \sum \overline{\frac{2p}{\mu Z}} \cdot \Delta p\ (\frac{psia^2}{cP})$
400	0.957	0.01312	63704.05649	31852.028	400	1.274E+07	1.2740E+07
800	0.932	0.01381	124290.1947	93997.126	400	3.760E+07	5.0339E+07
1200	0.912	0.01461	180162.1529	152226.174	400	6.089E+07	1.1123E+08
1600	0.897	0.01563	228267.2796	204214.716	400	8.169E+07	1.9292E+08
2000	0.887	0.01694	266195.189	247231.234	400	9.889E+07	2.9181E+08
2400	0.882	0.01858	292839.8274	279517.508	400	1.118E+08	4.0362E+08
2800	0.883	0.02058	308179.194	300509.511	400	1.202E+08	5.2382E+08
3200	0.889	0.02293	313910.6702	311044.932	400	1.244E+08	6.4824E+08
3600	0.901	0.02566	311452.0241	312681.347	400	1.251E+08	7.7331E+08
3400	0.918	0.02878	302756.8049	307104.414	400	1.228E+08	8.9615E+08
4400	0.942	0.03240	288337.2507	295547.028	400	1.182E+08	1.0144E+09
4800	0.972	0.03668	269291.5931	278814.422	400	1.115E+08	1.1259E+09
5200	1.012	0.04189	245351.2853	257321.439	400	1.029E+08	1.2288E+09
5600	1.062	0.04814	219059.7785	232205.532	400	9.288E+07	1.3217E+09
6000	1.119	0.05471	196029.7885	207544.783	400	8.302E+07	1.4047E+09
6074	1.13	0.05587	192422.4798	194226.134	74	1.430E+07	1.4190E+09
6400	1.17	0.05794	188820.9096	190621.695	326	6.221E+07	1.4812E+09
6800	1.218	0.06049	184579.7447	186700.327	400	7.468E+07	1.5559E+09
7200	1.266	0.06307	180352.5931	182466.169	400	7.299E+07	1.6289E+09
7600	1.314	0.06567	176155.4951	178254.044	400	7.130E+07	1.7002E+09
8000	1.362	0.06830	172002.2208	174078.858	400	6.963E+07	1.7698E+09
8400	1.41	0.07096	167905.4691	169953.845	400	6.798E+07	1.8378E+09
8800	1.457	0.07366	163988.1707	165946.820	400	6.638E+07	1.9042E+09
9200	1.505	0.07640	160027.8006	162007.986	400	6.480E+07	1.9690E+09
9600	1.552	0.07917	156251.047	158139.424	400	6.326E+07	2.0323E+09
10000	1.599	0.08199	152551.9992	154401.523	400	6.176E+07	2.0940E+09
10400	1.646	0.08485	148935.7055	150743.852	400	6.030E+07	2.1543E+09
10800	1.692	0.08774	145492.0594	147213.882	400	5.889E+07	2.2132E+09
11200	1.739	0.09068	142047.2756	143769.667	400	5.751E+07	2.2707E+09
11600	1.785	0.09366	138771.4671	140409.371	400	5.616E+07	2.3269E+09
12000	1.831	0.09668	135580.3728	137175.920	400	5.487E+07	2.3818E+09
12400	1.878	0.09974	132404.3743	133992.374	400	5.360E+07	2.4353E+09
12800	1.923	0.10283	129455.398	130929.886	400	5.237E+07	2.4877E+09
13200	1.969	0.10597	126521.6834	127988.541	400	5.120E+07	2.5389E+09
13600	2.015	0.10915	123672.9429	125097.313	400	5.004E+07	2.5890E+09
14000	2.061	0.11236	120908.2672	122290.605	400	4.892E+07	2.6379E+09
14400	2.106	0.11562	118282.4714	119595.369	400	4.784E+07	2.6857E+09
14800	2.151	0.11890	115733.1162	117007.794	400	4.680E+07	2.7325E+09
15200	2.197	0.12223	113207.3702	114470.243	400	4.579E+07	2.7783E+09
15600	2.242	0.12559	110808.9267	112008.148	400	4.480E+07	2.8231E+09

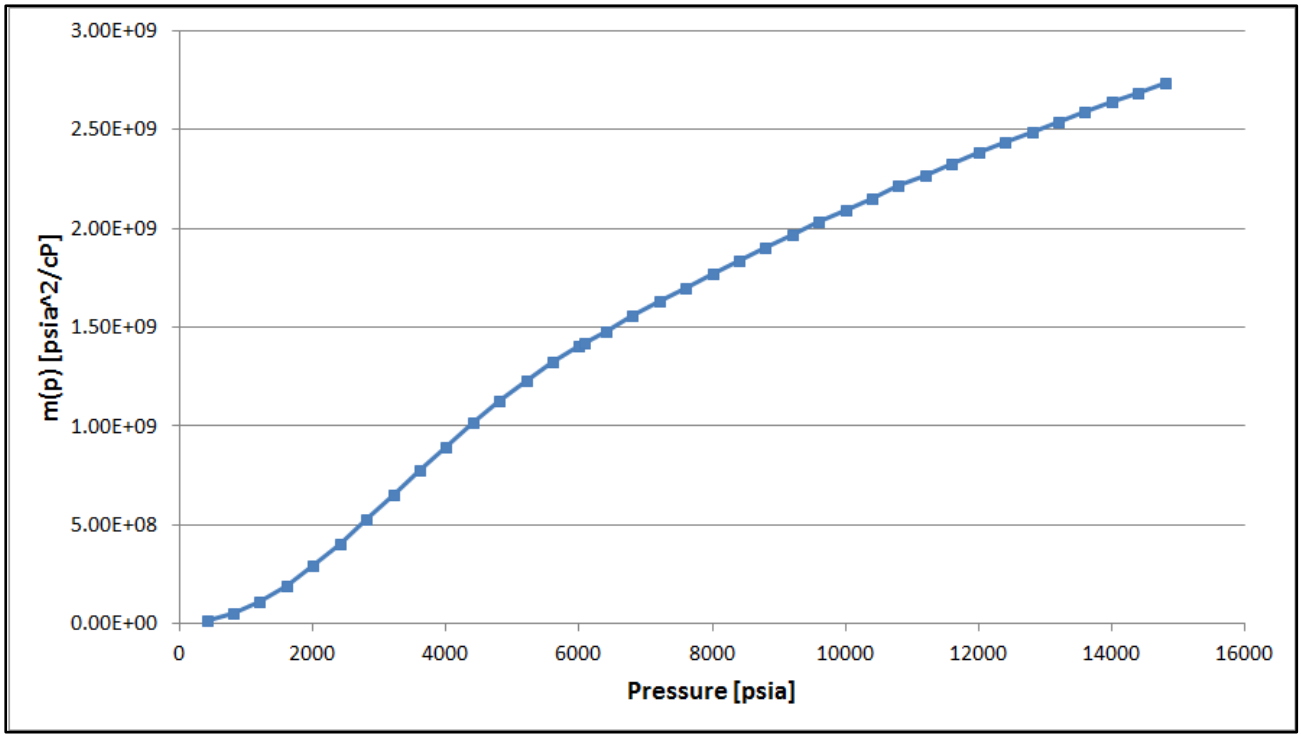

Figure 7: Real gas pseudo-pressure as a function of the real pressure.

3.4 Model Validity

To test the validity of the reservoir model, a simulation of a drawdown above the dew point in the infinite-acting period was performed in Eclipse 300. The initial reservoir pressure was set much larger than the fluid dew point pressure to make sure the gas condensate would behave as a single phase gas during the whole drawdown period. The surface-gas rate and the initial reservoir temperature was set to 2.50E6 Sm^3/d (88291.5 MScf/d) and 110 °C (689.67 °R) respectively. Reservoir permeability was set to 10 mD. After the simulation, m(p) versus ln(t) was plotted in a lin-lin plot as shown in **Figure 8** and the slope of the straight line could be calculated by Eq. (9):

$$m(p_i) - m(p_{wf}) = \frac{711QT}{kh} \tag{9}$$

where the slope, *m*, of the straight line in **Figure 8** in the infinite-acting period is given as:

$$m = \frac{m(p_{wf1}) - m(p_{wf2})}{\ln(t_2) - \ln(t_1)} \tag{10}$$

The infinite-acting period in field units can be expressed as:

$$t_{eia} = \frac{\varphi(\mu c_t)_i A}{0.000264k} \cdot (t_{DA})_{eia} \tag{11}$$

where the subscript *i* refers to initial reservoir conditions. Gas viscosity, μ_g, and total compressibility, c_t, were reported as output values from Eclipse 300 at initial reservoir conditions. For a circular geometry, $(t_{DA})_{eia} = 0.1$. The dimensionless time, t_D, can be expressed as:

$$t_D = \frac{0.000264 \cdot k \cdot t}{\varphi \cdot (c_t \mu)_i r_w^2} \tag{12}$$

where the product $c_t\mu$ is evaluated at initial reservoir pressure.

By choosing two values of pseudo pressures with the corresponding time values on the straight line in **Figure 8**, the flow capacity, *kh* and permeability, *k,* was calculated from the slope, *m*, by the rearrangement of Eq. (9). The permeability was calculated to be less than 5% deviation from the specified permeability of k=10mD in the Eclipse 300 input file.

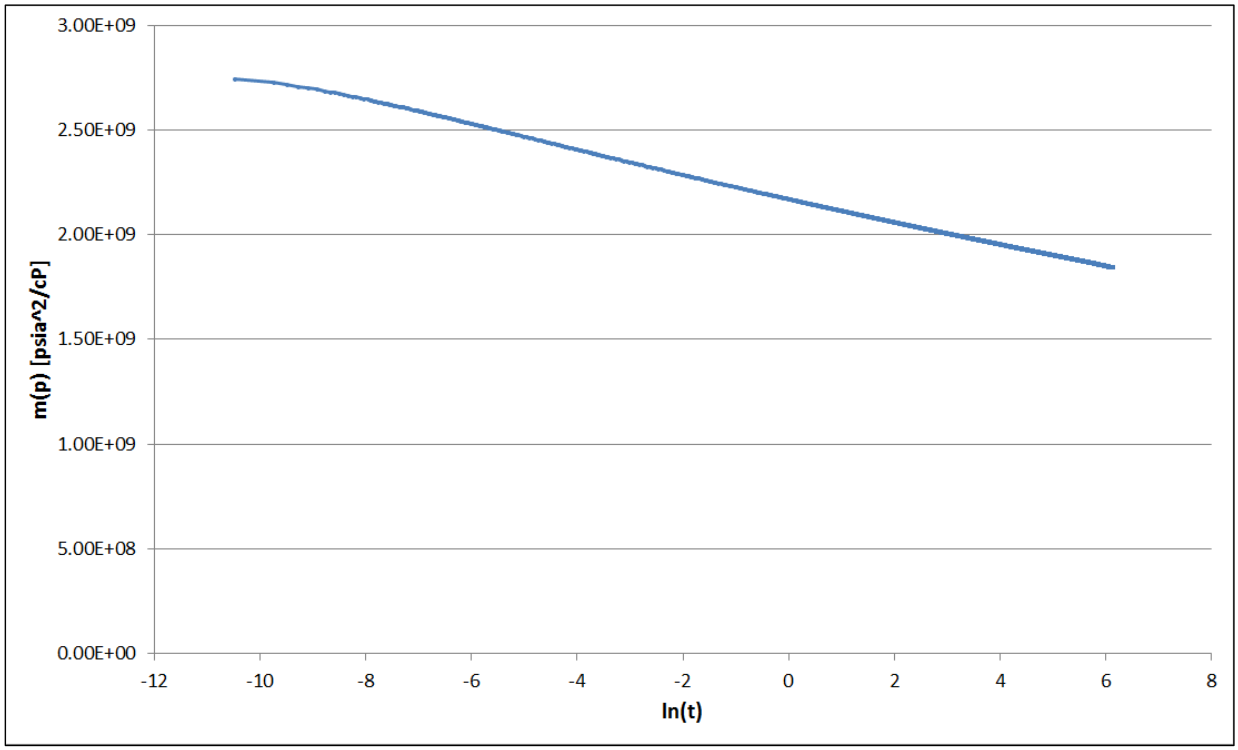

Figure 8: Lin-lin plot of pseudo-pressure versus ln(t) of a drawdown simulation above the dew point for a 2D, radial gas condensate reservoir model.

3.5 Eclipse 300 Simulation Test Cases

Test cases listed in **Table 7** and **Table 8** were prepared for a sequence of constant and changing surface gas rates, respectively. A simulated drawdown period of 1433 hours (≈60 days) corresponding to $(t_{DA})_{eia}$ = 0.096 was performed for all the cases in **Table 7**. Simulation run number one from **Table 7** started with an initial constant surface-gas rate of Q_g = 0.05E6 Sm^3/d. In the following cases in **Table 7** the gas rate was increased systematically with 0.05E6 Sm^3/d until a maximum gas rate of 0.50E6 Sm^3/d was used in case number ten. A maximum pressure change and maximum saturation change per time step in Eclipse 300 was set to 3 bar and 0.025 respectively.

Table 7: Test cases in Eclipse 300 with constant surface-gas rates.

Simulation Run No.	Q_g [1E6 Sm^3/d]	p_R [bar]	p_d [bar]	GOR_i [Sm^3/Sm^3]	$r_i = 1/GOR_i$ [Sm^3/Sm^3]
1	0.05	425	417.05	1078.78	0.00093
2	0.10	425	417.05	1078.78	0.00093
3	0.15	425	417.05	1078.78	0.00093
4	0.20	425	417.05	1078.78	0.00093
5	0.25	425	417.05	1078.78	0.00093
6	0.30	425	417.05	1078.78	0.00093
7	0.35	425	417.05	1078.78	0.00093
8	0.40	425	417.05	1078.78	0.00093
9	0.45	425	417.05	1078.78	0.00093
10	0.50	425	417.05	1078.78	0.00093

Table 8: Test cases in Eclipse 300 for schematic flow-rate sequences with rate changes.

Simulation test case A		Simulation test case B	
t	Q_g	t	Q_g
days	1E6 Sm^3/d	days	1E6 Sm^3/d
10	0.40	10	0.40
20	0.20	20	0.10
10	0 (shut in)	10	0 (shut in)
20	0.10	20	0.05

3.6 Gas-Oil Relative Permeability Curves Sensitivity

Figure 9 shows three different sets of gas-oil relative permeability curves. The gas-oil relative permeability curves for Set 1 (k_{ro} 1 and k_{rg} 1) were used as the base case. Gas-oil relative permeability curves for Set 2 (k_{ro} 2 and k_{rg} 2) and Set 3 (k_{ro} 3 and k_{rg} 3) were also used to investigate if the producing OGR could be sensitive to the gas-oil relative permeability curves. The relative permeability of gas in Set 2 and Set 3, share the same relative permeability to oil (k_{ro}) as k_{rg} in Set 1. The relative permeability to gas is less favorable for k_r Set 3 (triangles) and more favorable for k_r Set 2 (squares). Residual oil saturation, $S_{or,}$ and critical gas saturation, S_{gc}, were both set to zero. The gas-oil relative permeability curves were initially created by collected data in the vicinity of field Alpha. LET-correlations for oil and gas relative permeability presented by Lomeland et al. (2005) were used and are showed below in Eq. (13) and Eq. (14).

$$k_{rog} = k_{ro}(S_{wi}) \frac{(1 - S_{gn})^{L_o}}{(1 - S_{gn}) + E_o S_{gn}^{T_o}} \tag{13}$$

$$k_{rg} = k_{rg}^{o} \frac{S_{gn}^{L_g}}{S_{gn}^{L_g} + E_g (1 - S_{gn})^{T_g}} \tag{14}$$

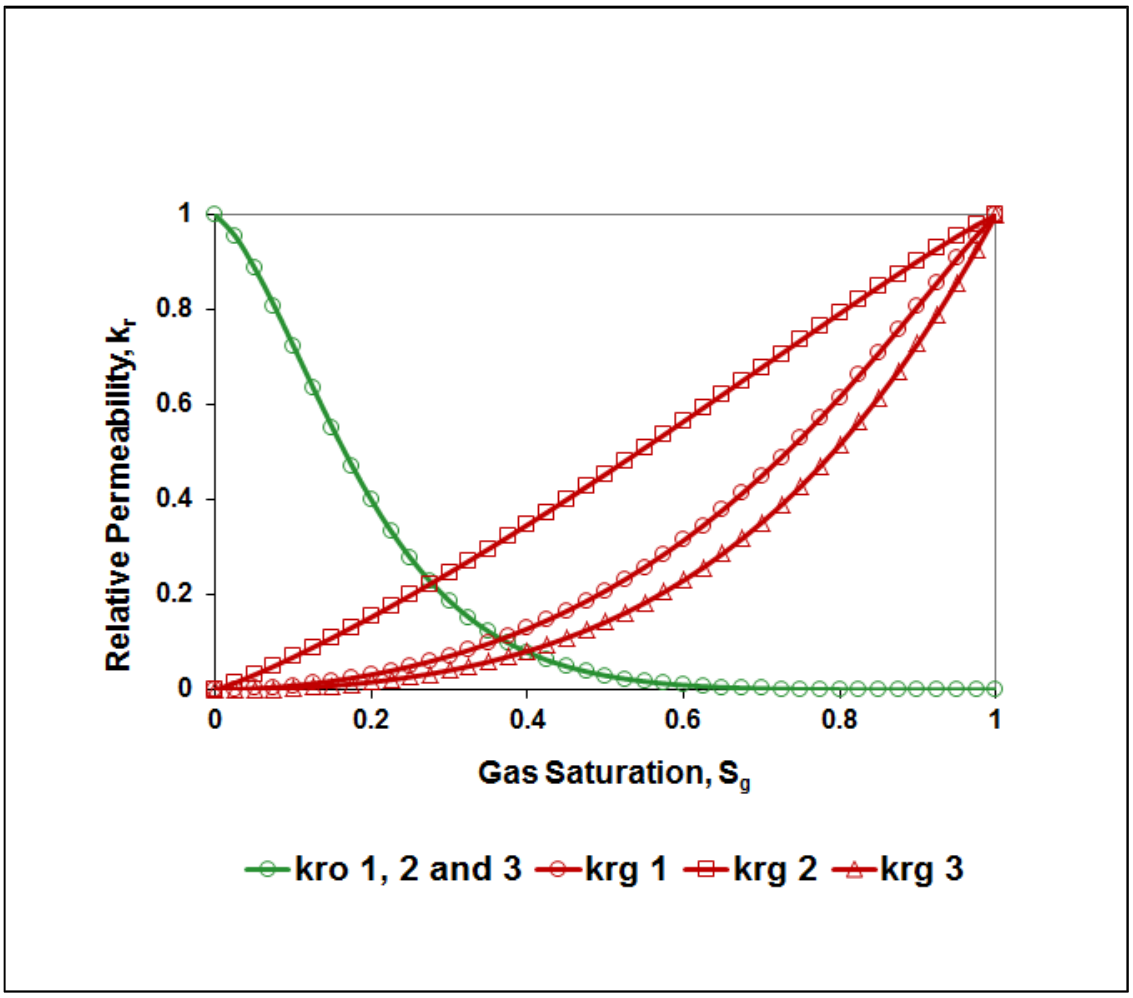

Figure 9: Three different sets of gas-oil relative permeability curves sharing the same k_{ro} curve.

4 Simulation Results

4.1 Constant Surface-Gas Rates

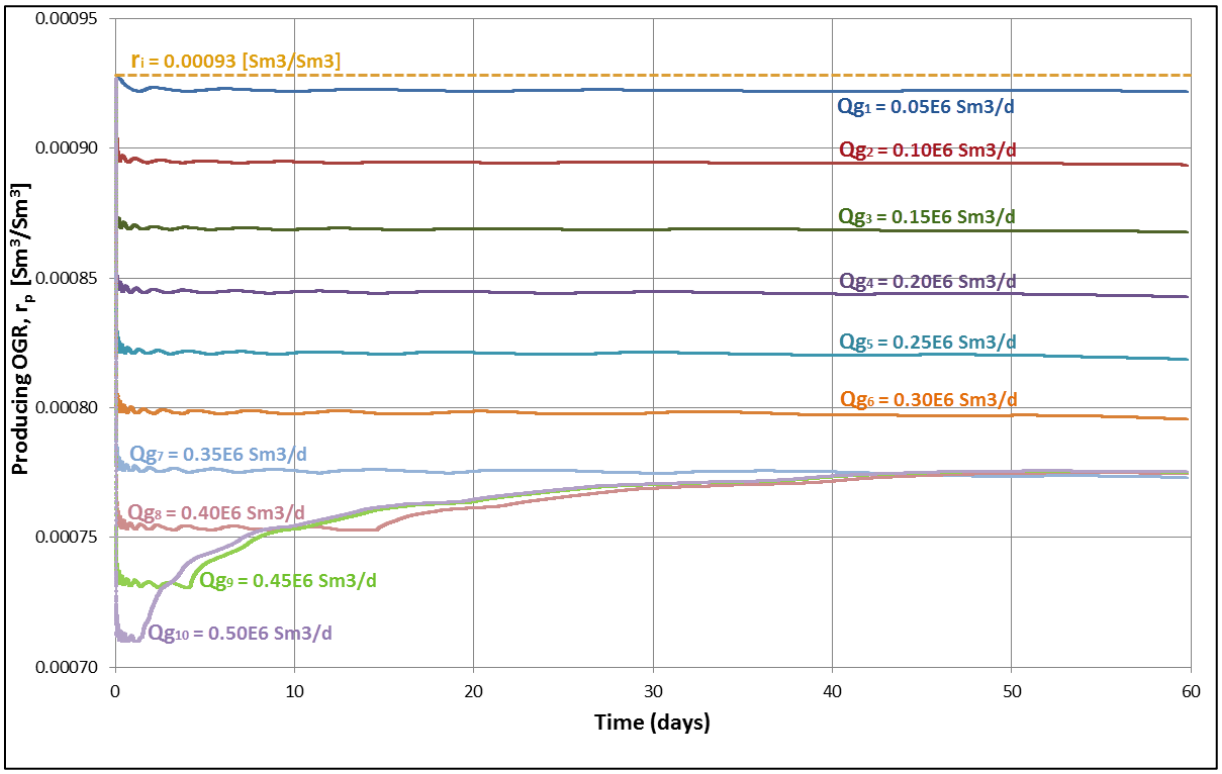

Figure 10: Producing OGR, r_p, behaviour with corresponding constant surface-gas rates, Q_g, vs. time during a drawdown of a vertical well below p_d in the infinite-acting period of a radial, 2D and compositional gas condensate reservoir model with k= 5mD.

Figure 10 shows the behaviour of the producing oil-gas ratio, r_p, of the rich gas condensate fluid below the dew point in the infinite acting period. Ten cases with different constant producing surface-gas rates during the infinite-acting period were simulated. In the cases with gas rates ranging from Qg_1=0.05E6 Sm^3 to Qg_7=0.35E6 Sm^3/d, r_p drops immediately below r_i, stabilizes and remains almost constant throughout the infinite-acting period. In the three last cases with Qg_8=0.40E6 Sm^3/d, Qg_9=0.45E6 Sm^3/d and Qg_{10}=0.50E6 Sm^3/d, the FBHP drops fast with high drawdown until a minimum specified BHP of 68.94 bar (≈1000 psia) is reached. In the cases with Qg_8, Qg_9 and Qg_{10}, r_p seems to increase to a value of approximately 0.00078 Sm^3/ Sm^3 as the well starts to produce with a minimum BHP

constraint. The producing OGR seems never to stabilize above the initial OGR for production with the ten test cases with constant gas rates.

Figure 11 shows the simulation results from **Figure 10** in dimensionless producing OGR, r_{pD} and dimensionless time, $t_{D,}$ using Eq. (12).

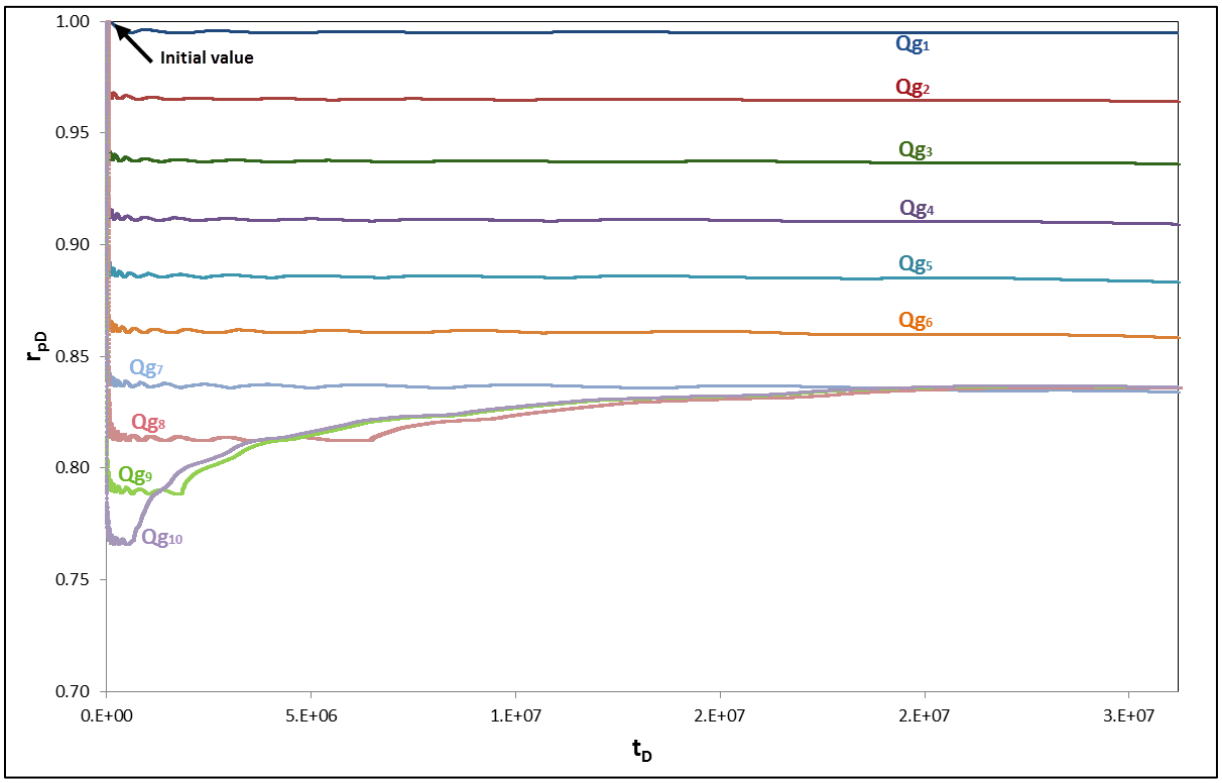

Figure 11: Dimensionless producing OGR, r_{pD}, with corresponding constant surface-gas rates, Q_g, vs. dimensionless time, t_D, in the infinite-acting period of a radial, 2D and compositional gas condensate reservoir model.

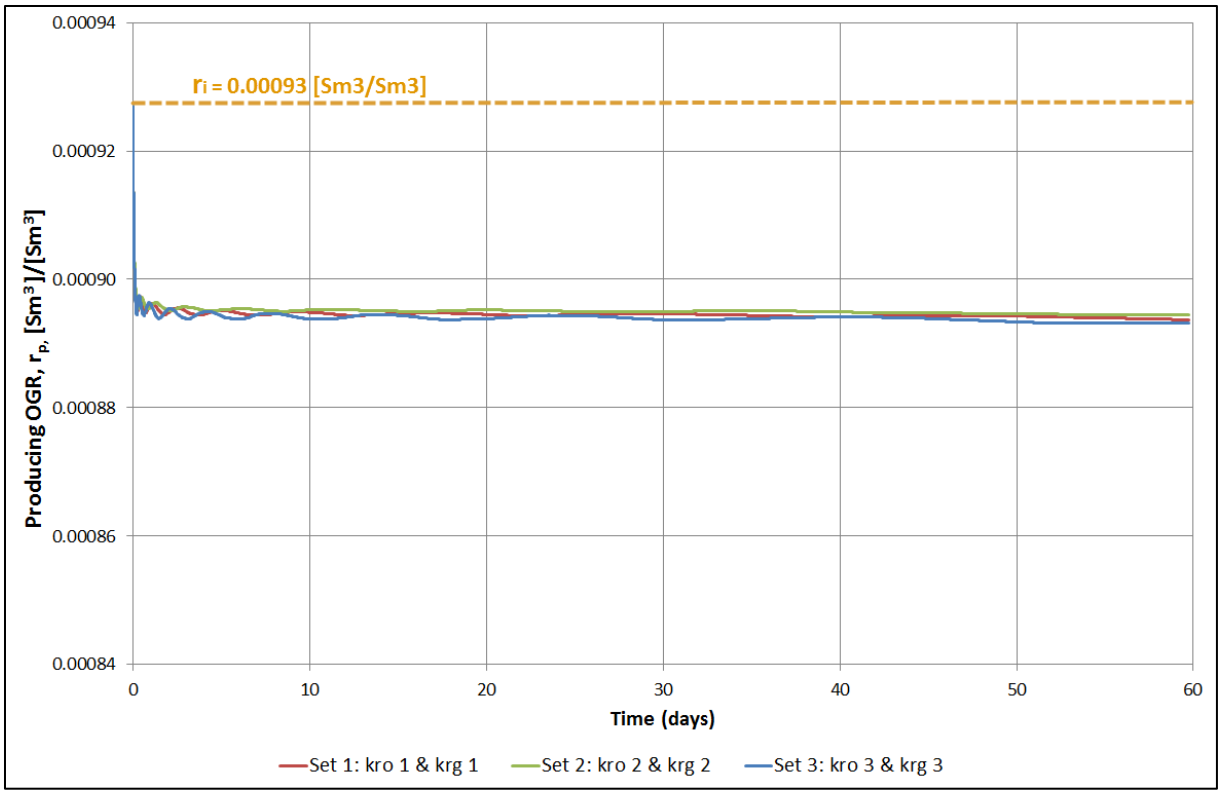

Figure 12: Producing OGR, r_p, vs time for three different sets of gas-oil relative permeability curves with constant Q_g = 100.000 Sm^3/d in the infinite-acting period of a radial, 2D compositional gas condensate reservoir model.

Figure 12 shows the behaviour of r_p with three different sets of gas-oil relative permeability curves presented in **Figure 9.** A new drawdown was simulated with a constant gas rate of Q_g= 100.000 Sm^3/d for each new set of gas-oil relative permeability curves. The difference in r_p between k_r Set 1, k_r Set 2 and k_r Set 3 was calculated to be approximately 0.13 %.

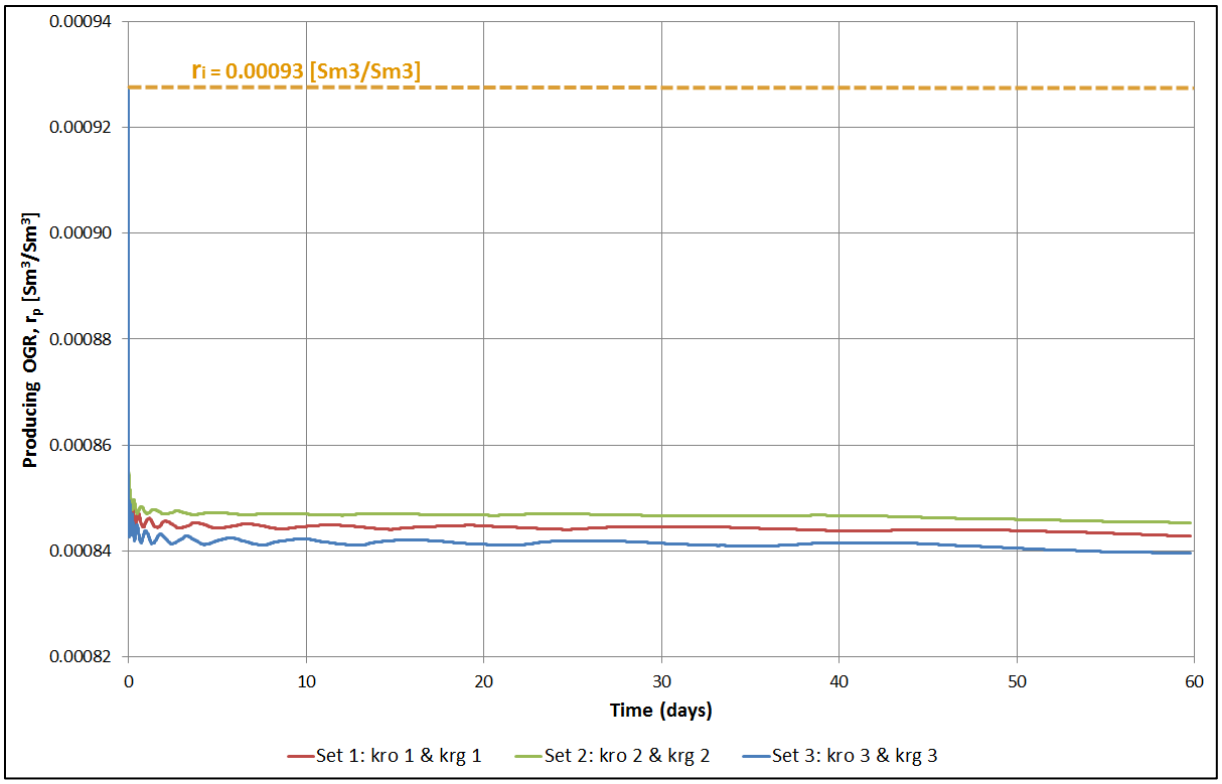

Figure 13: Producing OGR, r_p, vs time for three different sets of gas-oil relative permeability curves with constant Q_g = 200.000 Sm^3/d in the infinite-acting period of a radial, 2D compositional gas condensate reservoir model.

Figure 13 shows r_p with the three different sets of gas-oil relative permeability curves in the case when Q_g=200.000 Sm^3/d. The percentage deviation between k_r Set 2 and k_r Set 3 was calculated to be approximately 0.70%. As from **Figure 12,** a change in the gas relative permeability does not seem to change the behaviour of the producing OGR significantly.

4.2 Changing Surface-Gas Rates

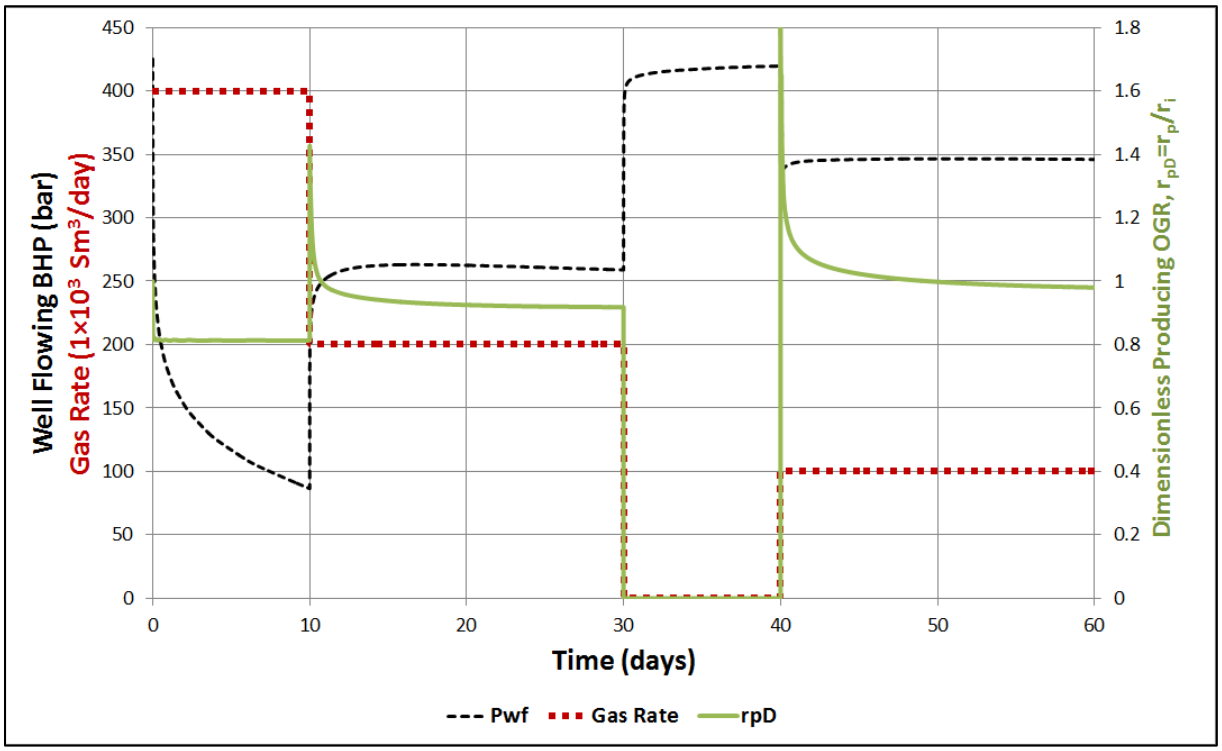

Figure 14: Simulated test case A: Dimensionless producing OGR, r_{pD}, vs. time using a 2D, radial compositional gas condensate reservoir model with gas rate changes: (a) 10 days at Q_g=400.000 Sm^3/d, (b) 20 days at Q_g=200.000 Sm^3/d, (c) 10 days shut in (Q_g=0 Sm^3/d), and (d) 20 days at Q_g= 100.000 Sm^3/d.

A dimensionless producing OGR (r_{pD}) is introduced in **Figure 14**. r_{pD} is defined as the ratio of producing OGR (r_p) to initial reservoir fluid OGR (r_i). **Figure 14** shows that during the first flow period of 10 days with a constant gas rate of Q_g = 0.40E6 Sm^3/d, r_{pD} drops immediately below the initial value (r_{pD}=1) and remains constant for a value of approximately r_{pD}=0.8. By an abrupt gas rate reduction to Q_g=0.20E6 Sm^3/d, r_{pD} immediately stabilize at new a value of approximately r_{rpD} =0.90 from day 10 to day 30. The very sharp increase of r_{pD} around day 10 and day 40 is probably only due to very abrupt changes in the Eclipse 300 simulations. At day 40, the gas rate was decreased to Q_g= 0.10E6 Sm^3/d and r_{pD} immediately increases before stabilizing around a value of r_{pD} = 1.

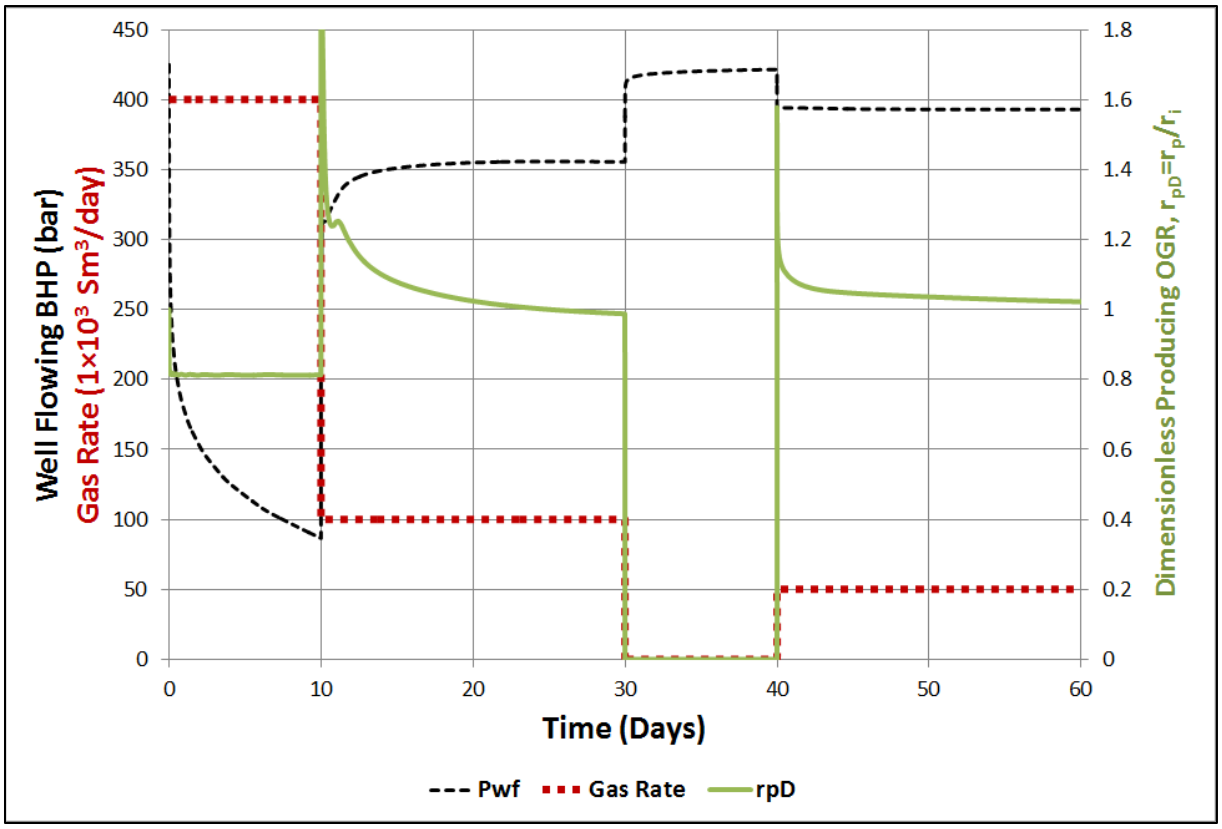

Figure 15: Simulated test case B: Dimensionless producing OGR, r_{pD}, vs. time in the infinite-acting period using a 2D, radial compositional gas condensate reservoir model with gas rate changes: (a) 10 days at Q_g=400.000 Sm^3/d, (b) 20 days at Q_g=100.000 Sm^3/d, (c) 10 days shut in (Q_g=0 Sm^3/d), and (d) 20 days at Q_g= 50.000 Sm^3/d.

Figure 15 shows the behaviour of r_{pD} versus time with 75 % and 87.5 % reduction of the initial gas rate in the periods day 10-30 and day 40-60, respectively. During the first flow period, r_{pD} remains constant. From day 10 the surface-gas rate is reduced to Q_g=0.10E6 Sm^3/d and r_{pD} immediately increases above r_{pD}=1, before decreasing and eventually stabilize around r_{pD}=1. After the shut in period on day 40, the gas rate is reduced from Q_g=0.10E6 Sm3/d to Q_g=0.05E6 Sm^3/d and it seems that r_{pD} stabilizes slightly above the initial value of r_{pD}=1 for the remaining 20 days of the infinite-acting period.

CHAPTER 5

5 Discussion and Conclusions

5.1 Discussion

Bøe et al. (1989) presented an analytical solution for infinite-acting constant GOR behaviour for a vertical well in a radial, 1D solution-gas drive reservoir. For long producing times, the producing GOR was derived to be a constant, independent of pressure and time. Compositional simulations performed in this study showed that for long producing times, (approximately 60 days), the producing OGR remained almost constant in the infinite-acting period for a radial, 2D and low permeable gas condensate reservoir when $p<p_d$. Thus, the producing OGR in this study seems to have the same analytical approach as the constant GOR behaviour theory presented by Bøe et al. (1989). Currently, no previous publications or reports have been found on the observation in this study. The compositional simulator has an equation of state formulation and has a slightly different way of treating the flow equations of oil and gas. But as long as the validity of the reservoir model was tested with good accuracy, the compositional simulations in this work would most likely give a good approximation to the analytical solution for infinite-acting constant GOR behaviour derived by Bøe et al. (1989).

Another observation in this work is that the producing OGR, r_p, never stabilized above the initial OGR for the test cases with constant flow-rates. Bøe et al. (1989) concluded that the stabilization level of the GOR could be higher or lower than the initial GOR, depending on the rate. In this study, it seemed that the producing OGR decreased from the initial OGR with increasing flow-rate. Several effects are involved when the wellstream flows towards the well below the dew point. The condensate originally dissolved in the gas phase drops out as liquid due to the pressure drop associated with the flow. Only condensate that drops out close to the wellbore reaches high enough saturation to flow into the wellbore, as discussed by Fevang (1995). As the flow-rate increases, more condensate drops out and flows towards

the well as a part of the oil phase. The gas phase loses some of the dissolved oil and thus becomes leaner. The gas saturation reduces and the relative permeability of gas decreases. Whether the producing OGR might stabilize above the initial OGR with increasing flow-rate is difficult to conclude.

The schematic sequences with changing rates show that the dimensionless producing OGR, r_{pD}, seems to stabilize and remain almost constant during the periods of changing flow-rates. r_{pD} also seems to stabilize at a new level associated with each new flow-rate. The behaviour of r_{pD} for the changing flow-rate sequences and r_p for the constant flow-rate cases seem both to be consistent and follow the analytical solution for constant GOR behaviour presented by Bøe et al. (1989).

Whitson et al. (2012) concluded that sampling in situ fluids from LRS reservoirs was very difficult and that the best strategy would be to collect separator samples early and at minimal drawdown. From the simulation results, one clearly observes that the producing OGR deviates from the initial OGR, depending on the rate. This would mean that it could be difficult to obtain a correct recombined oil and gas PVT sample from the gas condensate field of interest, if the stabilized producing OGR is different from the initial OGR.

5.2 Conclusions

This study has showed that for a low permeable gas condensate reservoir, the producing OGR dropped quickly, stabilized below the initial OGR and remained almost constant for long production times in the infinite acting period. The stabilization level of the producing OGR depended on the producing rate, but the producing OGR was never observed above the initial OGR. The producing OGR behavior for the low permeable gas condensate reservoir model in this study has not been found in previous literature. The conclusion is that an accurate recombined oil and gas PVT sample could be difficult to obtain in low permeable gas condensate reservoirs if the constant level of the producing OGR deviates from the initial OGR.

5.3 Suggestions to Further Work

- The work in this study should be tested with other gas condensate fluid compositions, ranging from lean to rich gas condensates.
- A skin factor could be included in the reservoir model.

References

Al-Hussainy, R., Ramey, H.J., Jr. and Crawford, P.B.: "The Flow of Real Gases Through Porous Media," *JPT* (May 1966) 624-636. *Trans*., AIME, 237.

Bøe, A., Skjæveland, S., and Whitson, C.H.: "Two-Phase Pressure Test Analysis," paper SPE 10224 presented at the 1981 SPE Annual Technical Conference and Exhibition, San Antonio, Oct. 5-7.

Coats, K. H.: "Simulations of Gas Condensate Reservoir Performance," JPT (Oct. 1985) 1870.

Dake, L.P.: *Fundamentals of Reservoir Engineering*, Elsevier Publishing, Oxford (1978).

Danesh, A.: *PVT and Phase Behaviour of Petroleum Reservoir Fluids*, Elsevier Publishing, Netherlands (1998).

El-Banbi, A.H., Cairo University/Schlumberger Holditch-Reservoir Technologies and McCain, Jr., W.D.: "Sampling Volatile Oil Wells," paper SPE 67232 presented at the SPE 2001 Production and Operations Symposium, Oklahoma City, Oklahoma, March. 24-27.

Fevang, Ø., and Whitson C.H.: "Modeling Gas-Condensate Well Deliverability," paper SPE 30714 first presented at the 1995 SPE Annual Technical Conference and Exhibition, Dallas, Oct. 22-25. Revised manuscript recieved 28 May 1996.

Fevang, Ø.: 1995, *Gas Condensate Flow Behavior and Sampling*, PhD thesis, Norges Tekniske Høgskole

Fevang, Ø., Singh, K., and Whitson, C.H.: "Guidelines for Choosing Compositional and Black-Oil Models for Volatile Oil and Gas-Condensate Reservoirs," paper SPE 63087 presented at the 2000 SPE Annual Technical Conference and Exhibition, Dallas, Texas, Oct. 1-4.

Lomeland, F., Ebeltoft, E., Thomas Hammervold, W., Statoil ASA, Stavanger, Petec Software & Services AS, Bergen, Norway.: "A New Versatile Relative Permeability Correlation", paper SCA2005-32 was prepared for presentation at the International Symposium of the Society of Core Analysts held in Toronto, Canada. 21-25 August 2005.

McCain Jr., W.D., and Alexander, R.A.: “Sampling Gas-Condensate Wells,” paper SPE 19729 presented at the 1989 SPE Annual Technical Conference and Exhibition, San Antonio, Oct. 8-11.

McCain, Jr, W.D.: 1990, *The Properties of Petroleum Fluids 2nd Edition,* PennWell Publishing Company, Tulsa, Oklahoma, USA.

Nagarajan, N.R., Honarpour, M.M., and Sampath, K.: “Reservoir Fluid Sampling and Characterization-Key to Efficient Reservoir Management,” paper SPE 101517 presented at the 2006 Abu Dhabi International Petroleum Exhibition and Conference, Abu Dhabi, U.A.E., Nov. 5-8.

Peres, M. M. A., Chapa-Macias, L., Serra, V.K., and Reynolds, A.C.: “Supplement to SPE 18530, Well-Conditioning Effects on Bubblepoint Pressure of Fluid Samples From Solution-Gas-Drive Reservoirs,” SPE 21478.

Peres, M. M. A., Macias-Chapa, L., Serra, V.K., and Reynolds, A.C.: “Well-Conditioning Effects on Bubblepoint Pressure of Fluid Samples from Solution-Gas-Drive Reservoirs,” paper SPE 18530 presented at the 1988 SPE Eastern Regional Meeting, Charleston, Nov. 1-4.

Reudelhuber, F.O.: “Sampling Procedures for Oil Reservoir Fluids,” JPT, 15-18 (Dec., 1957).

RP 44, *Recommended Practice for Sampling Petroleum Reservoir Fluids 2nd Edition*, API Dallas (2003).

Thomas, F.B., Anraku, T., and Bennion, D.W.: “Optimizing Production From A Rich Gas Condensate Reservoir,” paper SPE/DOE 35455 presented at the 1996 SPE/DOE Tenth Symposium on Improved Oil Recovery, Tulsa OK, April. 21-24.

Wall, C.G.: 1982, Characteristics of gas condensate reservoir and traditional production methods, *North Sea Gas Condensate Reservoirs and their Development 1982*, Oyez scientific and technical service, pp. 1-12.

Whitson, C.H., and Brulé, M.R.: 2000, *Phase Behaviour*, SPE monograph V. 20.

Whitson, C.H., Fevang, Ø., and Yang, T.: “Gas-Condensate PVT – What’s Really Important and Why?,” paper presented at the IBC Conference “Optimization of Gas Condensate Fields”, London, 28-29 January 1999.

Whitson, C.H and Sunjerga, S., PERA.: “PVT in Liquid-Rich Shale Reservoirs,” paper SPE 155499 presented at the 2012 SPE Annual Technical Conference and Exhibition, San Antonio, Oct. 8-10.

Whitson, C.H., and Torp, S.B.: “Evaluating Constant-Volume Depletion Data,” JPT (March 1983) 610-20.

Nomenclature

A	Reservoir drainage area, m^2 or ft^2
B_{gd}	Dry gas formation volume factor (FVF), *RB/Scf* or Sm^3/Sm^3
B_g	Gas formation volume factor, *RB/Scf* or Sm^3/Sm^3
B_o	Oil formation volume factor, *RB/STB* or Sm^3/Sm^3
c_t	Total compressibility, *bar* or $psia^{-1}$
E_g	Empirical parameter for gas phase
E_o	Empirical parameter for oil phase
h	Reservoir thickness, *m* or *ft*
k	Absolute permeability, *mD*
k_r	Relative permeability
k_{rg}	Gas relative permeability
k_{ro}	Oil relative permeability
kh	Flow capacity, *md·ft*
L_g	Empirical parameter for gas
L_o	Empirical parameter for oil
$m(p)$	Real gas pseudo-pressure, $psia^2/cP$
p_b	Bubble point pressure, *bar* or *psia*
p_c	Critical pressure, *bar*
p_d	Dew point pressure, *bar* or *psia*
p_{res}	Initial reservoir pressure, *bar* or *psia*
p_{sc}	Pressure at standard conditions, 1.01325 *bar* or 14.7 *psia*
p_{wf}	Flowing bottomhole pressure, *bar* or *psia*
p^*	Pressure at the boundary between Region 1 and Region 2
Q_g	Surface gas rate, Sm^3/d or *MScf/d*
r_e	External drainage radius, *m* or *ft*
r_i	Initial oil-gas ratio, Sm^3/Sm^3

r_p Producing OGR, Sm^3/Sm^3

r_{pD} Dimensionless producing OGR

r_s Oil dissolved in the gas phase, Sm^3/Sm^3

r_w Well radius, *m* or *ft*

R_s Gas dissolved in the oil phase, Sm^3/Sm^3

S Skin factor

S_{cc} Critical condensate saturation

S_g Gas saturation

S_{gc} Critical gas saturation

S_{gn} Gas saturation, normalized

S_{wi} Irreducible water saturation

Δr_s Difference between gas entering Region 1 and the gas flowing at a given radial distance from the wellbore

t Time, *days* or *hours*

t_{eia} Time to the end of the infinite-acting period, *days* or *hours*

t_D Dimensionless time

T_c Critical temperature, *°C*

T_{cri} Cricondentherm

T_g Empirical parameter for gas

T_o Empirical parameter for oil

T_{res} Reservoir temperature, *°C* or *°R*

T_{sc} Temperature at standard conditions, 15.56 *°C* or 60*°F*

v Molar volume

Z_g Gas Z-factor

Abbreviations

BHP	Bottom Hole Pressure, *bar* or *psia*
CVD	Constant Volume Depletion
EOS	Equation(s) of State(s)
FBHP	Flowing Bottom Hole Pressure, *bar* or *psia*
GOR	Gas-Oil Ratio, Sm^3/Sm^3
LRS	Liquid Rich Shale
OGR	Oil-Gas Ratio, Sm^3/Sm^3
SRK	Soave-Redlich-Kwong

Operators

Δ	difference

Subscripts

c	critical
d	dew point
D	dimensionless
DA	Dimensionless well drainage area
e	external
eia	end of the infinite-acting period
g	refers to gas phase
i	initial
o	refers to oil phase
p	producing
pD	dimensionless producing
res	reservoir
sc	standard conditions
t	total

w well

wf well flowing

Superscripts

***** Outer boundary

Symbols

ρ_g gas density

ρ_o oil density

μ_g gas viscosity, *cP*

μ_o oil viscosity, *cP*

φ porosity

γ Eulers constant